

Viability of using an embedded FBG sensor in a composite structure for dynamic strain measurement

Hang-yin Ling^a, Kin-tak Lau^{a,*}, Li Cheng^a, Wei Jin^b

^a Department of Mechanical Engineering, The Hong Kong Polytechnic University, Hung Hom, Hong Kong, China

^b Department of Electrical Engineering, The Hong Kong Polytechnic University, Hung Hom, Hong Kong, China

Received 28 February 2004; accepted 1 November 2005

Available online 5 January 2006

Abstract

In this paper, the utilisation of an embedded fibre-optic Bragg grating (FBG) sensor to measure dynamic strain of a clamped-clamped glass fibre composite beam is presented. A dynamic calibration test for strain measurement of the composite beam by the embedded FBG sensor and surface mounted strain gauge, at different vibration frequencies was conducted. Experimental results shown that the relationship between the photovoltage and strain measured by the embedded FBG sensor and strain gauge, respectively exhibited a linear fashion, when the strain value exceeded $1 \mu\epsilon$. Below this strain limit, the strain gauge could not precisely respond to the true strain of the beam. However, the signal extracted from the FBG sensor could truly reflect the strain of the beam at high vibration frequency condition. The first-two natural frequencies can be sharply indicated by a captured spectrum measured from the FBG sensor. Due to the out-of-plane vibration amplitude decreases with increasing the vibration frequency, the second natural frequency could not be clearly measured by the results extracted from the strain gauge.

© 2005 Elsevier Ltd. All rights reserved.

Keywords: Fibre-optic sensor; Smart structures; Measurement

1. Introduction

In the past decade, advanced composite materials have been widely used in a variety of load-bearing structures such as rotor blades, aircraft fuselage and wing structures. These structures are always subjected to unexpected external excitations at varied vibration frequency ranges. These dynamic interferences may cause the structures suffering

from fatigue damages and/or catastrophic failures due to the excitation frequency approaches to the natural frequency of the structures. Therefore, development of smart composite structures that comprises of integrated sensors, actuators and micro-processor(s) becomes a great challenge in this century. Fibre-optic Bragg grating (FBG) strain and temperature sensors have been broadly accepted as intrinsic structural health monitoring devices for measuring strains (mechanical and thermal), corrosion and vibration characteristics of smart composite structures [1–3]. The advantages of using the FBG sensors as embedded sensing devices of the

* Corresponding author. Tel.: +852 2766 7730; fax: +852 2365 4703.

E-mail address: mmkklau@polyu.edu.hk (K.-t. Lau).

composite structures include their small physical size, immunity of electromagnetic interference, lightweight, relative signal stability and suitability for wavelength multiplexing. Lau et al. [4] has proved that no significant mechanical degradation occurred when optical fibres were embedded into composite structures.

The principle of FBG technology is to measure the reflective signal that depends on the changes of spatial period and core refractive index in a grating region, of an optical fibre when it is subjected to elongations. If a FBG sensor is embedded into a composite structure, any change of the strain in the structure represent that the embedded fibre would be subjected to the same quantity of strains. Measuring the strains of the fibre results in reflecting the strains of the structures if a perfect bond between the fibre and composite is assumed [5].

For static strain measurement, Kang et al. [6] constructed a FBG sensor system to real-time monitor the strains of a filament wound composite tank. Lau et al. [7,8] also presented experimental studies on strain measurements using embedded FBG sensors in composite, concrete and composite-strengthened concrete structures. They found that the embedded FBG sensors could measure the true strain of the structures compared with externally bonded strain gauges, particularly at a region close to a crack tip or faces. James et al. [9] studied the transient response of gun barrel by using FBG sensors. They revealed that the accurate strain measurement could be maintained at any harsh mechanical and electromagnetic environments. One of our authors [10] also found that the FBG sensor technology could be used to measure the vibration characteristics of air flow. Davis et al. [11] measured the vibration mode shapes and identified the natural frequencies of composite beams using surface attached FBG sensors. However, only little attentions have been paid on dynamic strain measurements that truly respond to the mechanical performance of structures, on the use of the embedded FBG sensors.

This paper aims to experimentally study the feasibility of using an embedded FBG sensor, as a dynamic strain measuring device for a clamped-clamped composite beam subjected to an external excitation at different vibration frequency ranges. The principle of dynamic strain measurements with FBG sensor is discussed. A comparison of the results extracted from the FBG sensor and an externally bonded strain gauge is given.

1.1. Principle of dynamic strain measurement with FBG sensor

The principle of FBG strain sensor is to measure the change of reflected signal from a grating when it is subjected to elongation. This change would influence the reflective index (n_b) and spatial pitch Λ at the core section of this sensor [8]. According to the Bragg's law, the Bragg wavelength (λ_B) that is reflected from the sensor is given by

$$\lambda_B = 2n_b\Lambda \quad (1)$$

By neglecting the temperature effect of the sensor, the relationship between the reflective Bragg wavelength shift ($\Delta\lambda_B$) corresponding to the change of strain at the grating region ($\Delta\varepsilon_g$) can be expressed as

$$\Delta\lambda_B = K\Delta\varepsilon_g \quad (2)$$

where K is the theoretical gauge constant. In the static strain measurement, the constant “ K ” can be measured by conducting a traditional tensile test. A schematic illustration of a FBG strain measuring system is shown in Fig. 1. Light is emitted from a superluminescent light emitting diodes (SLED) system to a coupler which acts as a Y-type channel to guide the emissive light to the FBG sensor and the reflective signal back to an optical tuneable filter (OTF). Photodetector and signal analyser are then used to detect the power output of the reflected light and convert the final signal into voltage quantity in real time, respectively. Owing to the dependence of the photodetector output denoted by photovoltage-variation (ΔV_{photo}) and the wavelength shift ($\Delta\lambda_B$) when the signal passes through the OTF

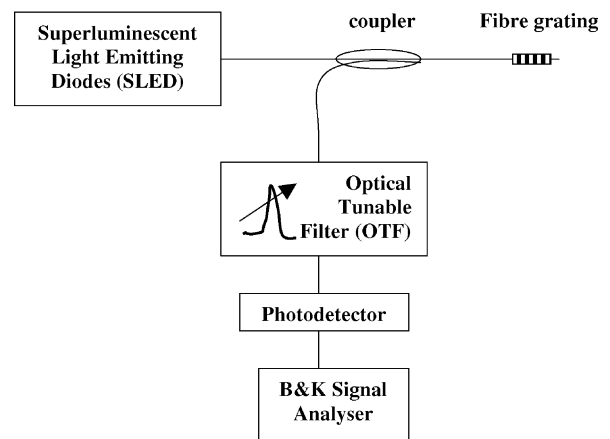


Fig. 1. FBG strain measuring system.

transmitted spectrum as shown in Fig. 2, the linear relationship between the photovoltage (ΔV_{photo}) and the wavelength shift ($\Delta\lambda_{\text{B}}$) is obtained. This relationship can be expressed as

$$\Delta V_{\text{photo}} = C\Delta\lambda_{\text{B}} \quad (3)$$

where C is the proportional constant which depends on the designable system. Most recent literatures have relied on the calibration factor K that is experimentally measured by a static tensile test to represent the strain of structures under dynamic condition. However, up to the best knowledge from the authors, no reports have indicated the reliability of this factor for the dynamic strain measurement.

By combining Eqs. (2) and (3), a following equation is formed:

$$\Delta V_{\text{photo}} = S\Delta\varepsilon_{\text{g}} \quad (4)$$

where $S = C \cdot K$ is an arbitrary constant of the FBG strain measuring system presented in this paper. A conversion factor S shown in Eq. (4) have to be determined through a dynamic calibration test to accurately measure the strain of a beam by using an embedded FBG sensor. It is reminded that the photodetector output is related to the power of the SLED and the power loss of the above FBG measurement set up such as the reflectivity of grating, splice loss of fibre, insertion loss of TOF and the power splitting reduction through the coupler.

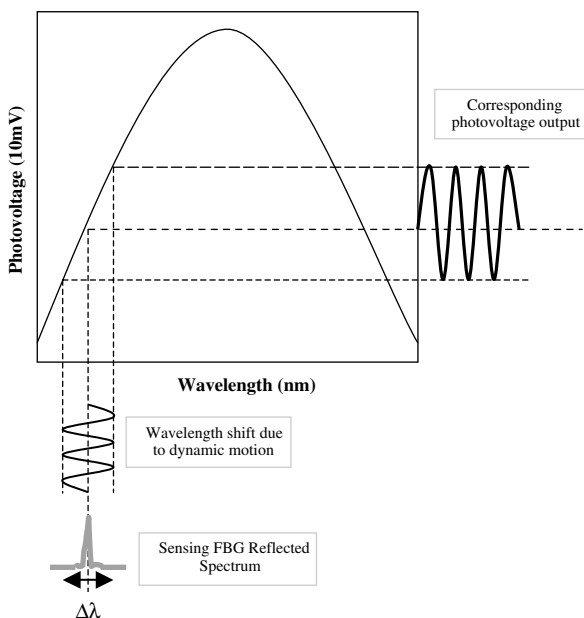


Fig. 2. Dependence of photovoltage and wavelength shift.

Additionally, it is more convenience to detect the photovoltage output by using a signal analyser than that of an optical spectrum analyser (OSA). The dynamics strain measurement as the real time photovoltage signal can be seen directly through this signal analyser without involving any complicated mathematical manipulations.

1.2. Experiments on dynamic strain measurement

A calibration test of a clamped-clamped glass fibre composite beam with an embedded FBG sensor, subjected to an out-of-plate vibration motion at different frequency ranges, was conducted. Ten layers of $0^\circ/90^\circ$ E-glass fabric and Epoxy-based resin (Araldite MY 750) were used to fabricate the glass fibre composite beam. A single optical fibre with pre-written grating sensor was embedded into the composite beam during the lay up process. The physical and mechanical properties of the beam are listed in Table 1. The Young's modulus and Poisson ratio of the beam were measured according to ASTM D3039. As the resonance effects are interested, the first-two natural frequencies were measured by the Bruel&Kjaer (B&K) piezoelectric accelerometer in the frequency range of 10–250 Hz.

Table 1
Physical and mechanical properties of the beam

Physical properties	Mechanical properties		
Mass	25.3 g	Young Modulus	13.363 GPa
Thickness	2.3 mm	Poisson Ratio	0.14
Length	305 mm	1st and 2nd natural	80 Hz and 230 Hz
Width	25 mm	Frequencies	

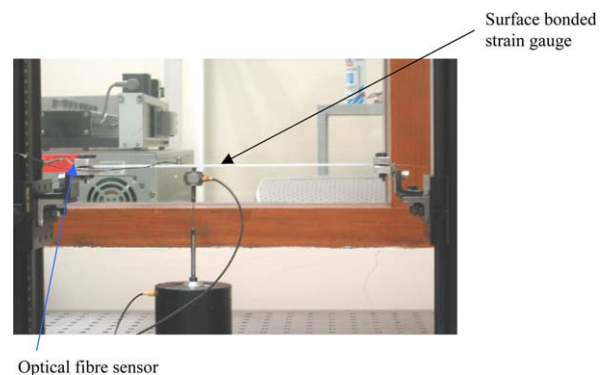


Fig. 3. Composite beam embedded with FBG sensor and surface mounted strain gauge.

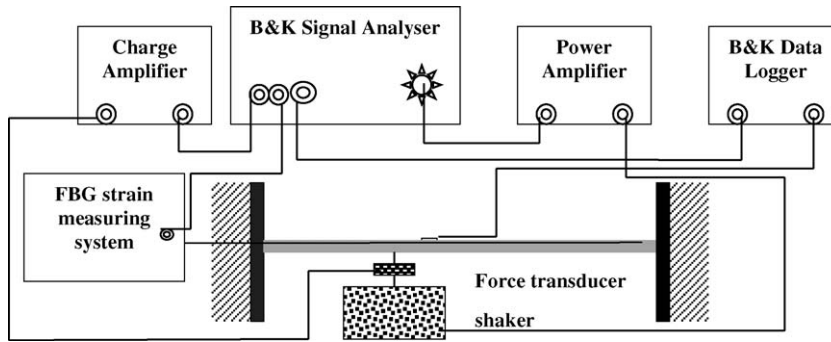


Fig. 4. The whole experimental setup.

Figs. 3 and 4 show the composite beam with the embedded FBG sensor and a surface bonded strain gauge on its corresponding surface and an experiment setup of this study, respectively. The beam was clamped rigidly at both ends. An electric-driven shaker, used to generate external excitations to the beam, is attached to the bottom of the beam at a position 100 mm from the left end as indicated in the figure. A force transducer was placed between the shaker’s stinger and the beam. The photovoltage and strain measured by the embedded sensor and strain gauge were recorded simultaneously.

2. Results and discussion

Frequency response functions within a low frequency range of 10–250 Hz recorded by a strain gauge and a FBG sensor are plotted in Fig. 5. Obviously, the trend of both curves is similar. The results

from the FBG sensor show the peak sharply of the first-two natural frequency modes, 80 Hz and 230 Hz. However, the second peak shown by the strain gauge becomes vague. At a frequency range below 100 Hz, it was found that the relation in strains measured from the both devices was apparently in proportion. However, an intersection between these curves is found at a frequency of 110 Hz. Beyond this limit, the strains measured by the strain gauge maintained at very fluctuating values ($2 \pm 1 \mu\epsilon$) until it reached a frequency of 230 Hz, where was an expected natural frequency of the second vibrating mode of the beam. However, the results from the FBG sensors remained maintaining a constant reading at a frequency range between 140 Hz and 200 Hz. Moreover, the symmetric responses at the two natural frequency modes were observed by the FBG sensor whereas this phenomenon could not be shown by the strain gauge.

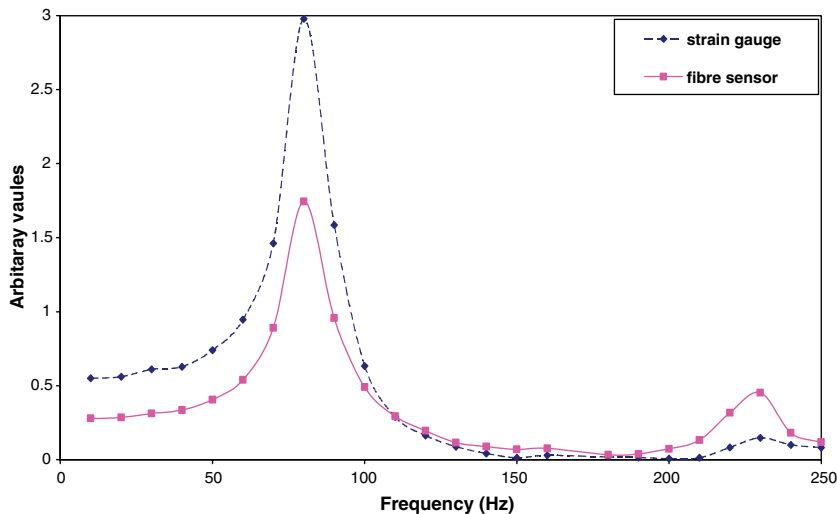


Fig. 5. Frequency response functions of FBG sensor and strain gauge.

Based on the captured spectrums shown by these two strain measuring devices, it is obviously seen that at the first region where the frequency range below 100 Hz, the responses from these two devices are proportional and comparable. However, the fluctuating results from the strain gauge was observed in a frequency range between 110 Hz and 200 Hz. After the frequency reaching to 210 Hz, the increases of the normalized strain and photovoltage were found. According to these phenomena, it is reasonable to compare these three different regions separately. In Fig. 6a, the relationship between the photovoltage and strain measured by the FBG sensor and strain gauge, respectively at

the frequency range below 100 Hz is shown. In the figure, the linear correlation between the photovoltage and strain is found and the conversion factor S shown in Eq. (4) was calculated as 0.5898. However, this linear proportional fashion cannot be maintained from all strains measured by the strain gauge at the strain level below $3 \mu\epsilon$. In Figs. 6b and 6c, the plots of the strain measured by the strain gauge against photovoltage in the second and third regions are shown. In these two figures, due to the incorrect strain measurements from the strain gauges, the corresponding linear correlations appeared in Fig. 6a between the measured photovoltage and strain do not exist.

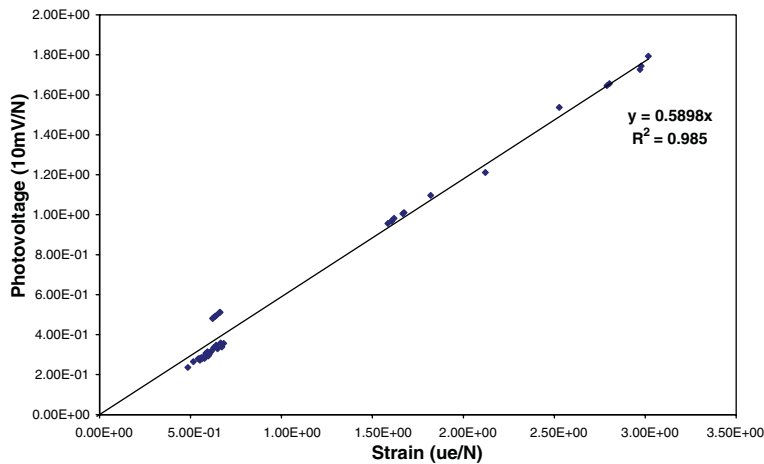


Fig. 6a. Correlation of normalized photovoltage and strain at the frequency range between 10 and 100 Hz.

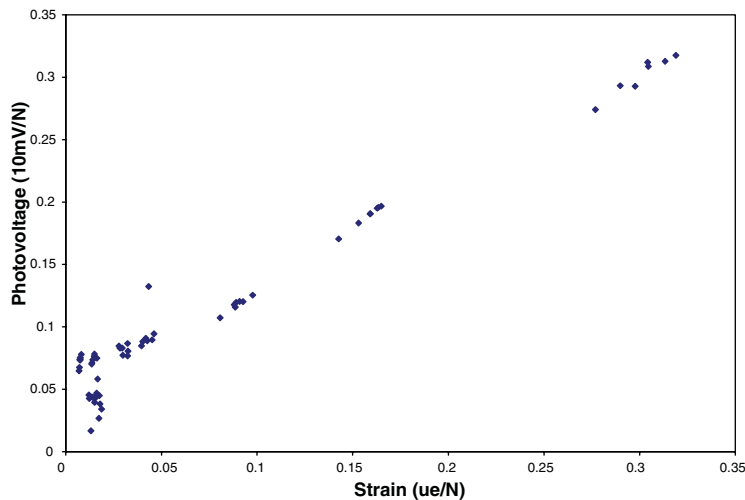


Fig. 6b. Correlation of normalized photovoltage and strain at the frequency range between 110 and 200 Hz.

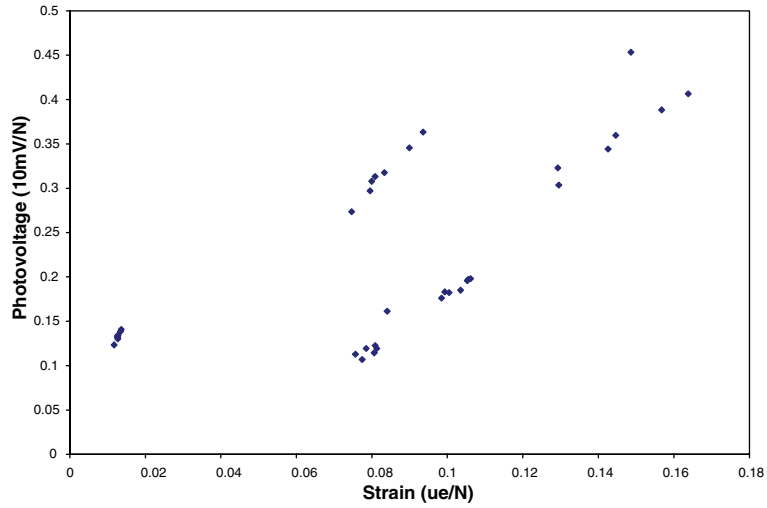


Fig. 6c. Correlation of normalized photovoltage and strain at the frequency range between 210 and 250 Hz.

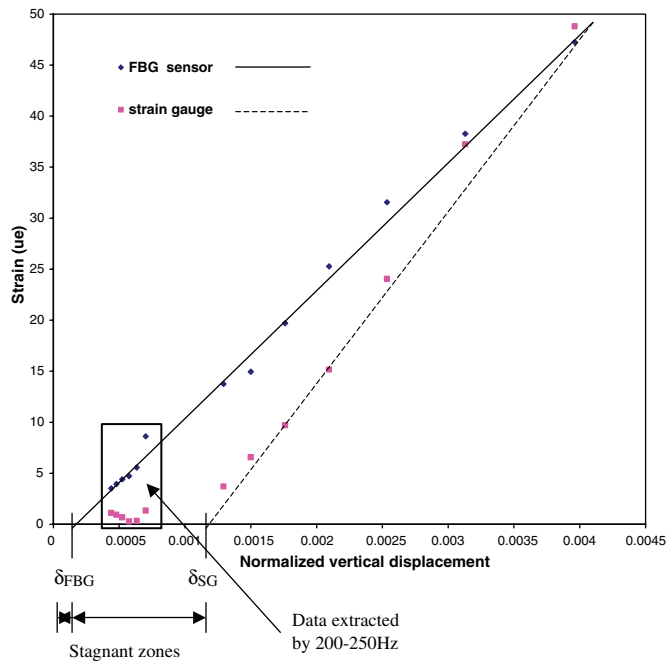


Fig. 7. Graph of actual strain against normalized vertical displacement.

In Fig. 7, a comparison of the strains calculated by Eq. (4) using the results from the FBG sensor and measured by strain gauge is shown. In this figure, it is obvious that no strain was measured by the strain gauge below the normalised vertical displacement that represents the out-of-plane vibration amplitude, of 0.0011, δ_{SG} . According to the in situ strain measuring results, this limit corre-

sponded to the beam’s surface strain of $1 \mu\epsilon$ in which the strain value is smaller than the sensitivity of the strain gauge. Due to the delay of the strain measurement by using the strain gauge and FBG sensor, at the regions below δ_{SG} and δ_{FBG} respectively, these zero strain regions are called “stagnant zones”. It is clear that the length of the stagnant zone of δ_{SG} is comparatively larger than that of

δ_{FBG} . Besides, the results extracted from the FBG sensors in a frequency range between 200 Hz and 250 Hz also agree well to a fitted line shown in the figure. In view of this phenomenon, it is concluded that the use of the embedded FBG could provide more reliable and accurate dynamic strain measurement at high vibration frequency condition.

3. Conclusion

Dynamic strain measurement of a clamped-clamped composite beam by using an embedded FBG sensor and a surface mounted strain gauge is presented. The embedded FBG sensor could accurately measure the first-two, may be even more natural frequencies of the beam. Two sharper peaks were shown in an in situ captured spectrum. However, the second peak could not be shown clearly by the results from the strain gauge. Dynamic calibration test indicated that the viability of using the FBG sensor to measure strain at high frequency range. A large stagnant zone existed for the strain measured by the strain gauge. However, the existence of the stagnant zone obtained by the FBG sensor is trivial. This paper emphasises on the dynamic strain measurement using the embedded FBG sensor for composite structures. In fact, many works have been done recently regarding to the use of embedded FBG sensors for identifying the natural frequency mode and damping responses of structures, less emphasis was paid on structural dynamic strain monitoring, which in turn provides important information to the structural behaviour and mechanical performance of the structures. In most practical cases, the failure of structures may not be merely caused by the instability due to the excitation frequency approaches to the natural frequency of the structures. Fatigue damage is one of the major causes of structural failure of the structures. The real time dynamic strain monitoring could provide a full stress profile that allows periodical evalu-

ation of the fatigue life, and thus maintain a high level of safety of the structures.

Acknowledgement

This project was fully supported by The Hong Kong Polytechnic University Grants (PolyU 5192/05E) and (A-PF34).

References

- [1] K.S.C. Kuang, R. Kenny, M.P. Whelan, W.J. Canrwell, P.R. Chalker, Embedded fibre Bragg grating sensors in advanced composite materials, *Compos. Sci. Technol.* 61 (2001) 1379–1387.
- [2] P. Ferdinand, S. Magne, V.D. Marty, S. Rougeault, L. Maurin, Applications of fiber Bragg grating sensors in the composite industry, *MRS Bull.* 27 (5) (2002) 400–407.
- [3] Y.L. Lo, F.Y. Xiao, Measurement of corrosion and temperature using a single pitch Bragg grating fibre sensor, *J. Intell. Mater. Sys. Struct.* 9 (1998) 800–807.
- [4] K.T. Lau, C.C. Chan, L.M. Zhou, W. Jin, Strain monitoring in composite-strengthened concrete structures using optical fibre sensors, *Composites: Part B* 32 (2001) 33–45.
- [5] K.T. Lau, L.B. Yuan, L.M. Zhou, Thermal effects on embedded grating sensor for FRP structure, *Smart Mater. Struct.* 10 (2001) 705–712.
- [6] H.K. Kang, J.S. Park, D.H. Kang, C.U. Kim, C.S. Hong, C.G. Kim, Strain monitoring of a filament wound composite tank using fibre Bragg grating sensors, *Smart Mater. Struct.* 11 (2002) 848–853.
- [7] K.T. Lau, L.M. Zhou, L.B. Yuan, C.H. Woo, Strain monitoring in FRP laminates and concrete beam using FBG sensors, *Compos. Struct.* 51 (2000) 9–20.
- [8] K.T. Lau, Fibre-optic sensors and smart composites for concrete applications: a review article, *Magn. Concr. Res.* 55 (1) (2003) 19–34.
- [9] S.W. James, R.P. Tatam, S.R. Fuller, C. Crompton, Monitoring transient strains in a gun barrel using fibre Bragg-grating sensors, *Meas. Sci. Technol.* 10 (1999) 63–67.
- [10] W. Jin, Y. Zhou, P.K.C. Chan, H.G. Xu, A fibre-optic grating sensor for study of flow-induced vibrations, *Sens. Actuators* 79 (2000) 36–45.
- [11] M.A. Davis, A.D. Kersey, J. Sirkis, E.J. Friebele, Shape and vibration mode sensing using a fibre optic Bragg grating array, *Smart Mater. Struct.* 5 (1996) 759–765.